A numerical procedure for failure mode detection of masonry arches reinforced with fiber reinforced polymeric materials

A numerical procedure for failure mode detection of masonry arches reinforced with fiber reinforced polymeric materials

S Galassi

Department of Architecture, Section of Materials and Structures, University of Florence, Piazza Brunelleschi 6, 50121 Florence, Italy

E-mail: stefano.galassi@unifi.it

Abstract. In this paper a mechanical model of masonry arches strengthened with fibre-reinforced composite materials and the relevant numerical procedure for the analysis are proposed. The arch is modelled by using an assemblage of rigid blocks that are connected together and, also to the supporting structures, by mortar joints. The presence of the reinforcement, usually a sheet placed at the intrados or the extrados, prevents the occurrence of cracks that could activate possible collapse mechanisms, due to tensile failure of the mortar joints. Therefore, in a reinforced arch failure generally occurs in a different way from the URM arch. The numerical procedure proposed checks, as a function of an external incremental load, the inner stress state in the arch, in the reinforcement and in the adhesive layer. In so doing, it then provides a prediction of failure modes. Results obtained from experimental tests, carried out on four in-scale models performed in a laboratory, have been compared with those provided by the numerical procedure, implemented in *ArchiVAULT,* a software developed by the author. In this regard, the numerical procedure is an extension of previous works. Although additional experimental investigations are necessary, these former results confirm that the proposed numerical procedure is promising.

1. Introduction

In recent years innovative materials and techniques [1-6] for strengthening and repairing architectural and monumental heritage constructions [7,8], as well as ruins in the archaeological sites [9], have been widely used. In particular, masonry arches and vaults have been successfully strengthened using composite materials applied at the intrados or the extrados. For the analysis of these structures, the author has recently presented new numerical tools [10-15].

The intervention of strengthening or consolidation made using composite materials is more targeted and less invasive in comparison to the traditional technologies and materials employed in the recent past. Among the advantages of using these materials, it is worth mentioning the following FRP properties: lightness, high resistance, high elastic modulus and stiffness, reduced costs due to the ease of transport and assembly, minimal invasiveness, rapid installment in the structure, reversibility of the intervention.

Composite materials and masonry are very compatible [16] (such as in the case of concrete reinforced by steel) and each of these two materials offers particular performance and strengths in the structure: the masonry supports compressive forces, while tensile forces, which cannot be supported by the masonry, are diverted to the fibers, which are designed specifically to perform this function. The reinforced masonry is, in turn, configured as an innovative material, thus its design must consider

all possible failure modes, that may occur, which are different from the standard masonry failure ones. More specifically, the following five states should be verified:

- Equilibrium of the structure,
- Compressive force in the masonry,
- Shear force in the mortar joints,
- Adhesion between the reinforcement and the structure,
- Tensile force in the reinforcements.

According to the limit analysis laws, the following five limits correspond to the above mentioned states and, in order to guarantee safety, they must not be exceeded:

- Collapse mechanism or tensile cracks,
- Crushing of the masonry,
- Sliding of one brick upon another in correspondence of the mortar joints,
- Delamination, often a "rip-off failure", that is a failure of the union between masonry and the reinforcement, on the side of masonry (removal of part of the brick),
- FRP rupture.

According to the strength hierarchy criterion, the design of the reinforcement should be aimed at predicting, choosing and preferring one particular failure mode over the others. Consequently, one can select which type of composite and adhesive is better to use, the cross section of the reinforcement and its placement on the substrate, always relying on the tensile strength of the fibers and compressive strength of the masonry. For the assessment of the behaviour of a masonry arch reinforced with FRP materials, the few numerical procedures available in the literature take into account only some failure modes [17,18]. Therefore, a targeted mechanical model and numerical procedure are herein proposed. The tool discussed below is an extension of previous works [19,20] that, in the current formulation, allows one to detect the most probable failure mode of a reinforced arch.

2. Mechanical model

The mechanical model of a masonry arch (figure 1) is assumed to be composed of a finite number of rigid-blocks assembled by elastic mortar joints. In the mortar joints, all the elasticity (i.e.: deformability) of the arch is concentrated. Mortar joints are modeled, in a discrete way, by a device composed of four links orthogonal to the mid-surface of the joint, plus an additional link arranged along that surface.

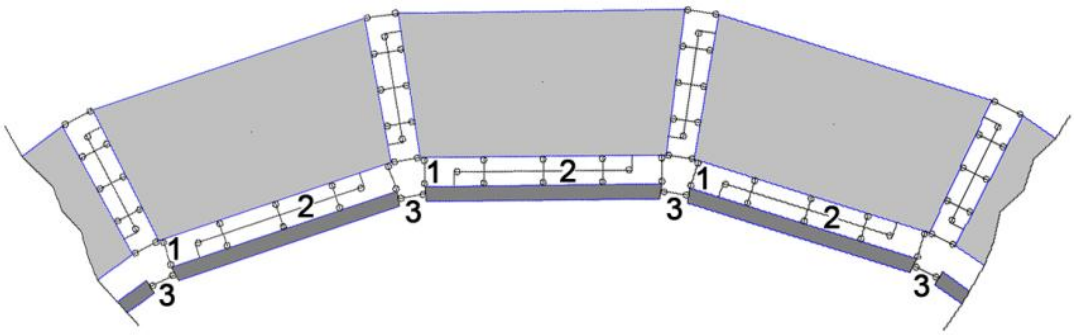

Figure 1. Mechanical model of the reinforced arch: mortar, adhesive and FRP links.

In order to consider the main aspects of the relationship between structure and reinforcement, the latter is assumed to be composed of "frp-type" elements equal to the number of masonry blocks, with their weight, although negligible, linked together and to the structure. The FRP elements are placed at the intrados or extrados of the arch and are also assumed to be rigid.

The interface which connects fiber with the structure is modeled by a device composed of one set of links, capable of transmitting compressive forces and low tensile forces (type 1 links) and an additional link, capable of transmitting the shear force (type 2 link).

The joint linking one reinforcement element with the next one is composed of one link, capable of transmitting only a tensile force (type 3 link). In type 3 links all the elasticity of the reinforcement is assumed to be concentrated. The first and the last links simulate "external constraints", that is "links with the first structural element unreinforced"; therefore, they represent the so-called "anchorage length".

Type 1 links measure the peeling forces, and they are the tensile forces responsible for the delamination failure which is due to the typical curvilinear shape of the arch (in the case of reinforcements placed at the intrados). However, the reinforcement detachment can also be provoked by the loss of adhesion, which is checked through type 2 links. Indeed, type 3 links, provide, interface by interface, the local tensile force in the reinforcement, and give information about the possibility of its rupture if it exceeds the FRP tensile strength.

3. Numerical procedure

The numerical procedure for the analysis of a reinforced rigid-block arch, modeled in the discrete way described above, is based on the formulation of the set of the equilibrium equations and the elastic-kinematic equations, which are expressed in matrix form in equation (1):

$$\begin{cases} \mathrm{AX} = \mathrm{F} + \alpha F' \\ \widetilde{\mathrm{A}}\mathrm{x} + \mathrm{KX} = \Delta \end{cases} \tag{1}$$

where {F} is the vector of the dead loads acting on the structure, {F'} is the vector of the additional loads that are increased by the incremental load factor α, {X} is the vector of the unknown forces in the links of the joints, [A] is the equilibrium matrix whose coefficients are a function of the block shape and the slope of the joints, $[\widetilde{A}]$ is the kinematic matrix, {x} is the vector of the displacements of the block centers of mass and [K] is the matrix whose coefficients are populated by the deformability of mortar, adhesive and FRP links. Vector {Δ}, the "impressed distortion vector", is the key to checking the possible aforementioned failure modes, which are caused by the failure of some joint links.

In the hypothesis that for dead loads F and very low additional forces αF' (i.e.: low values of α) the masonry arch and the reinforcement are undamaged, the solution of equation 1 is provided by the linear elastic solution in equation (2):

$$\mathrm{X}_0 = \mathrm{K}^{-1}\widetilde{\mathrm{A}}(\mathrm{AK}^{-1}\widetilde{\mathrm{A}})^{-1} \cdot (\mathrm{F} + \alpha\mathrm{F}') \tag{2}$$

Equation (2) is obtained from equation (1) assuming vector {Δ}={0}.

During the analysis the value of α is increased step by step and, in correspondence to each value, the five limit states, listed in the introduction section, can no longer be verified. These limits are expressed by inequalities in equation (3), that are constraints on equation (1):

$$\begin{cases} \mathrm{M}^{(-)} \le \mathrm{X}_{\mathrm{n,j}}^{(\mathrm{m})} \le 0 \text{ (on mortar axial links)} \\ \mathrm{X}_{\mathrm{t}}^{(\mathrm{j})} \le \mathrm{f} \cdot \sum_{\mathrm{j}=1}^{4} \mathrm{X}_{\mathrm{n,j}}^{(\mathrm{m})} \text{ (on mortar tangent links)} \\ 0 \le \mathrm{X}_{\mathrm{j}}^{(1)} \le \mathrm{G}^{(+)} \text{ (on adhesive axial links)} \\ \left|\mathrm{X}_{\mathrm{j}}^{(2)}\right| \le \mathrm{G} \text{ (on adhesive tangent links)} \\ \mathrm{X}_{\mathrm{j}}^{(3)} \le \mathrm{L} \text{ (on FRP links)} \end{cases} \tag{3}$$

According to the five inequalities in equation (3), to predict the failure modes the algorithm introduces a distortion coefficient [21] in the link whose force, at the current step of the analysis, does not respect the corresponding inequality. The distortion provokes the failure of that link. In detail, the

distortions act on tense mortar axial links (provoking tensile cracks), on mortar axial links that are compressed more than their compression strength limit expressed by $M^{(-)}$ in equation (3) (provoking the crushing of masonry), on the mortar tangential links whose shear force exceeds the friction force expressed by the second of equation (3) according to the Coulomb's friction criterion [22,23] (sliding of blocks occurrence), on the "adhesive links" type 1 stretched more than the limit $G^{(+)}$ (delamination occurrence), and on "FRP links" type 3 stretched more than the FRP strength L (FRP rupture occurrence). In this framework, the term "adhesive links" is only symbolic and should be properly considered as "masonry links": in fact, it has been demonstrated that delamination does not occur in the adhesive layer but, rather, inside the masonry, with its consequent ripping [24-28]. Therefore, it is more convenient and correct to consider the rupture limit tension $G^{(+)}$ of such links by referring to the brick rupture limit tension rather than to the adhesive one, which is much higher.

The insertion of a distortion coefficient in a link provokes a modification of the inner stress state and therefore, the static solution vector must be recomputed. The solution vector that also takes into account the effect of the distortion is provided in equation (4):

$$X = X_0 + \left(I - K^{-1}\tilde{A}\left(AK^{-1}\tilde{A}\right)^{-1}A\right)\cdot\Delta \tag{4}$$

At the end of the iterative nonlinear analysis, the load-bearing capacity of the reinforced arch, as well as its failure mode, are assessed, providing information on the intermediate failures in correspondence to each value of the incremental loads. In such a way the numerical procedure provides guidance on the more targeted strengthening intervention of an existing masonry arch as a function of the expected serviceability loads.

4. Numerical and experimental results

To assess the reliability of the numerical procedure proposed above, four models of masonry arches reinforced with carbon FRP composites in scale 1:2 have been performed at the Official Laboratory for Testing of Materials and Structures of the Department of Architecture at the University of Florence (Italy). Experimental results have been compared with the results provided by the numerical procedure.

Such models reproduced a segmental arch with a 150 cm spam, an internal radius corresponding to 86.5 cm, with fixed imposts and inclined by 30° and a square cross section corresponding to 10 x 10 cm.

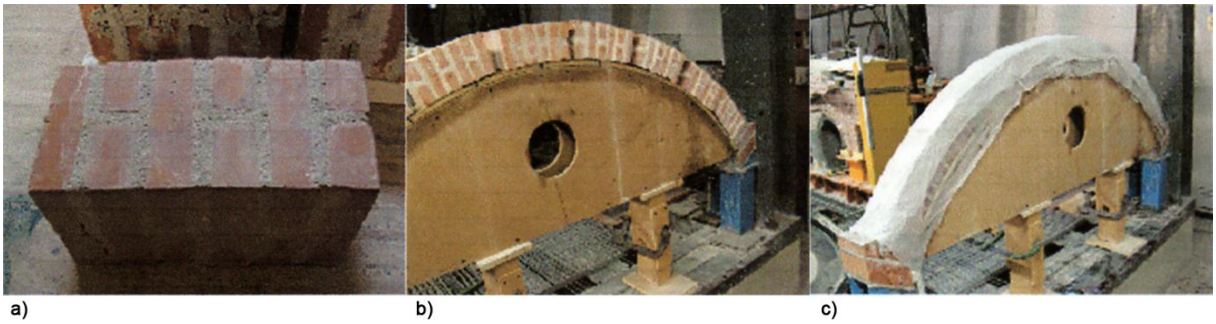

Figure 2. Construction phases: (a) macro-block; (b) assemblage of macro-blocks on the centering; and (c) curing under a layer of wet paper.

Each arch has been built for subsequent phases. First, some "macro-blocks" of 6 bricks have been bonded, following the intrados curve of the arch to be built (figure 2(a)). After 28 days of curing, they have been positioned on the centering and bonded together so as to obtain the whole arch (figure 2(b)). Finally, the arch has been covered with a layer of wet paper and left to cure for 10 days in order to avoid the occurrence of micro-cracks due to drying and shrinkage (figure 2(c)).

The right and left impost sections have not been laid directly on the testing machine but on bricks adequately shaped and placed in such a way as to simulate the heads of two fixed pillars (figure 3(a)).

The experimental trial was conducted by simulating an increasing point force at the keystone using a hydraulic jack which impressed an increasing vertical displacement. In correspondence to a load of 1980 N the first crack at the keystone appeared and then, later, at the haunches at a load of 2630 N. In correspondence to a load of 4320 N the delamination process began, and, starting from the keystone sections, this process involved little by little, the sections near the left haunch removing part of the masonry (figure 3(b)).

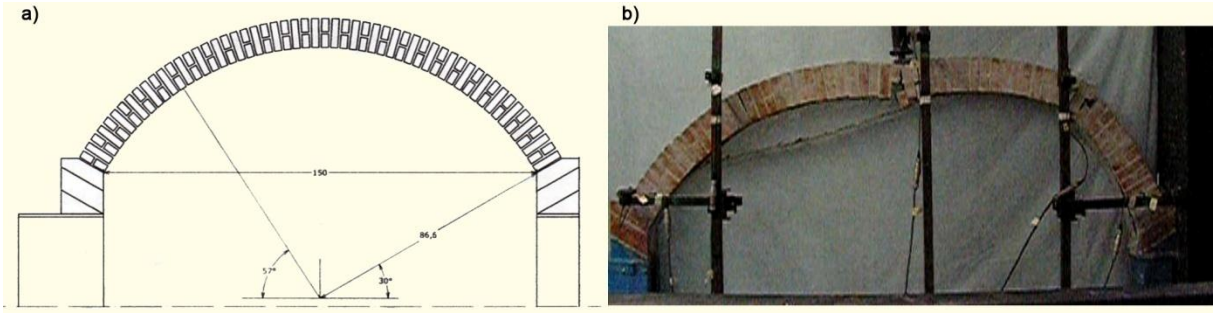

Figure 3. (a) Geometry of arch models performed in a laboratory; and (b) Experimental trial.

In the numerical model the action of the hydraulic jack at the keystone of the arch was simulated inputting two equal point forces at the centre of gravity of both the keystone blocks. During the analysis, these forces were increased little by little.

The numerical model showed (figure 4), step by step, the misshaping delamination process which also occurred experimentally. It highlighted a peak load of the same level as well as the cracking pattern that occurred experimentally, which highlighted both mortar joint failure due to tensile forces and the position of the reinforcement detached in many intrados interfaces.

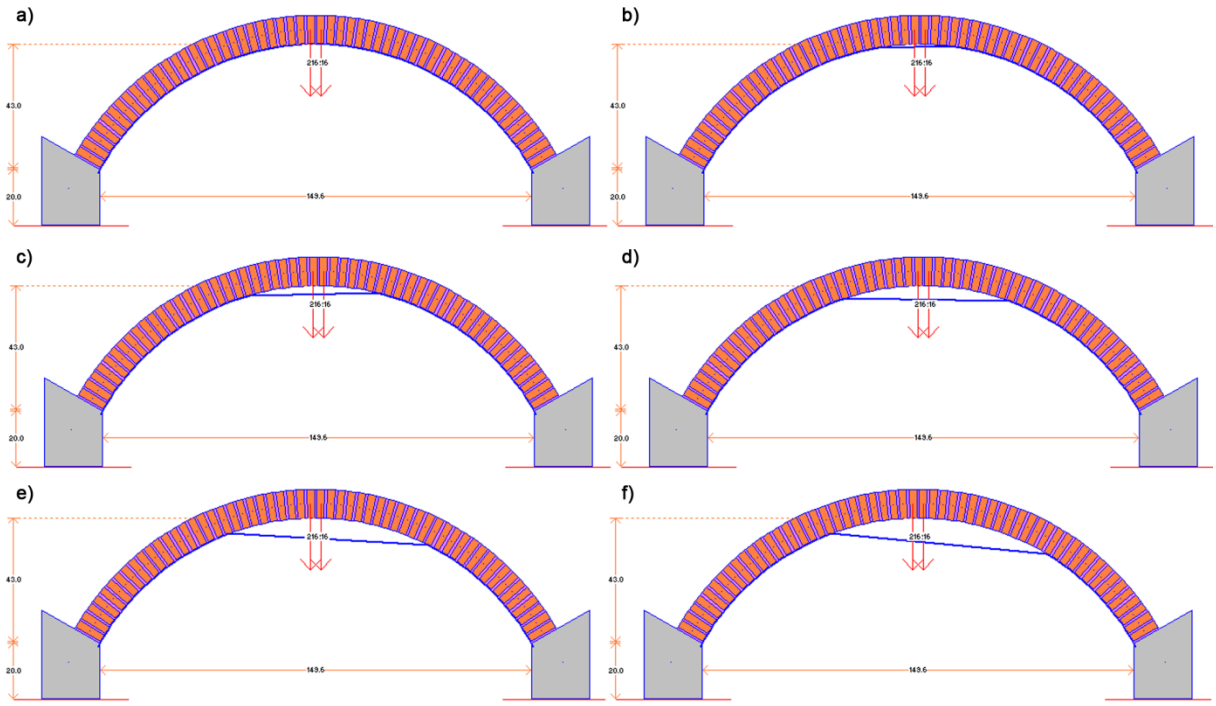

Figure 4. Delamination process computed by the software *ArchiVAULT*.

5. Conclusions

Failure modes of an arch reinforced with FRP materials are different from the typical failure modes of an URM one. For this reason, a nonlinear numerical procedure for the analysis of failure modes, that is an extension of that presented in a previous work, has been described in more detail in this paper and also implemented in the software *ArchiVAULT*, in such a way as to provide a user-friendly design tool for engineers.

In order to provide prediction of failure modes, five limit states have been considered in the proposed procedure. Since the discrete model has been assumed for interpreting the mechanical behaviour of the arch, such limit states are checked in correspondence to the mortar, adhesive and FRP joints.

According to the strength hierarchy criterion, this tool is aimed at providing guidance on a targeted design of the reinforcement system in order to avoid irreversible failure modes, such as masonry crushing, and phenomena that could lead to instant collapse, such as the FRP rupture.

Even if additional investigations should be performed on a higher number of experimental models, the comparison between numerical results and the results of the in laboratory experimental arches seems to confirm the reliability of the procedure proposed.

Acknowledgments

Architect Daniela Sinicropi, that performed the experimental trial in our laboratory, is gratefully acknowledged.

References

[1] Paradiso M, Galassi S, Borri A and Sinicropi D 2013 "Reticolatus": an innovative reinforcement for irregular masonry. A numeric model, *Structures and Architecture: Concepts, Applications and Challenges*, *Proc. 2nd Int. Conf. on Structure & Architecture ICSA2013,* Paulo J S Cruz (Ed.) (London: CRC Press/Balkema, Taylor and Francis Group), Guimaraes, Portugal

[2] Alecci V, Focacci F, Rovero L, Stipo G and De Stefano M 2017 Intrados strengthening of brick masonry arches with PBO–FRCM composites: experimental and analytical investigations *Compos. Struct.* **176** 898-909

[3] Alecci V, De Stefano M, Focacci F, Luciano R, Rovero L and Stipo G 2017 Strengthening masonry arches with lime-based mortar composite *Buildings* **7** 49

[4] Fagone M and Ranocchiai G 2017 An experimental analysis of the mechanical behaviour of cnchored CFRP-to-masonry reinforcements loaded by out-of-plane actions *Key Eng. Mat.* **747** 204-11

[5] Jurina L 2016 Experimental tests on consolidation of masonry bridges using "ram-reinforced arch method" *Proc. IIX Int. Conf. on Arch Bridges* (5-7 October 2016, Wroclaw, Poland)

[6] Borri A, Castori G and Corradi M 2011 Intrados strengthening of brick masonry arches with composite materials *Compos. Part B-Eng.* **42** 1164-72

[7] Galassi S, Dipasquale L, Ruggieri N and Tempesta G 2018 Andalusian timber roof structure in Chefchaouen, Northern Morocco: construction technique and structural behavior *ASCE's Journal of Architectural Engineering* **24** 10.1061/(ASCE)AE.1943-5568.0000315

[8] Paradiso M, Galassi S and Benedetti S 2014 The peculiar defensive fort of San Fernando de Bocachica, Colombia *Patologia della Costruccion, Tecnologia de la Rehabilitacion y Gestion del Patrimonio, Proc. Latin American Congress on Construction Pathology, Rehabilitation Technology and Heritage Management (Rehabend 2014),* Luis Villegas, Ignacio lombillo, Clara Liano, Haydee Blanco (Eds.), Gráficas Iguña, S.A., Santander, Spain, (in Italian)

[9] Ruggieri N, Galassi S and Tempesta G 2018 Pompeii's Stabian Baths. Mechanical behaviour assessment of selected masonry structures during the 1st century seismic events *Int. J. Archit. Herit.* 10.1080/15583058.2017.1422571

[10] Galassi S, Misseri G, Rovero L and Tempesta G 2017 Equilibrium analysis of masonry domes. On the analytical interpretation of the Eddy-Lévy graphical method *Int. J. Archit. Herit.* **11** 1195-211
[11] Galassi S and Tempesta G 2017 Analysis of masonry block structures with unilateral frictional joints *Proc. of Int. Conf. on Electronic, Control, Automation and Mechanical Engineering (ECAME 2017)* (19-20 November 2017, Sanya, China), *DEStech Transactions on Engineering and Technology Research* 246-51 10.12783/dtetr/ecame2017/18396
[12] Pugi F and Galassi S 2013 Seismic analysis of masonry voussoir arches according to the Italian building code *Ing. Sismica-Ital.* **30** 33-55
[13] Paradiso M, Galassi S and Benedetti S 2014 Stability of masonry arches and vaults: traditional methods and automatic calculation *Patologia della Costruccion, Tecnologia de la Rehabilitacion y Gestion del Patrimonio, Proc. Latin American Congress on Construction Pathology, Rehabilitation Technology and Heritage Management (Rehabend 2014),* Luis Villegas, Ignacio lombillo, Clara Liano, Haydee Blanco (Eds.), Gráficas Iguña, S.A., Santander, Spain (in Italian)
[14] Alecci V, De Stefano M, Galassi S, Lapi M and Orlando M 2018 An assessment of American criterion for detecting plan irregularity *Proc. of 8th European Workshop on the Seismic Behaviour of Irregular and Complex Structures (8EWICS)* (19-20 October 2017, Bucharest, Romania) (in press)
[15] Galassi S, Misseri G, Rovero L and Tempesta G 2018 Failure modes prediction of masonry voussoir arches on moving supports *Eng. Struct.* (in press)
[16] Sinicropi D, Perria E, Galassi S, Paradiso M and Borri A 2014 Artificial aging of mortar prisms reinforced through steel, glass and organic fibers *Key Eng. Mat.*, A Di Tommaso, C Gentilini and G Castellazzi (Eds.) **624** 542-50
[17] Briccoli Bati S, Fagone M and Rotunno T 2013 Lower bound limit analysis of masonry arches with CFRP reinforcements: A numerical method *Journal of Composites for Construction* **17** 10.1061/(asce)cc.1943-5614.0000350
[18] Caporale A, Luciano R and Rosati L 2006 Limit analysis of masonry arches with externally bonded FRP reinforcements *Comput. Method Appl. M.* **196** 247-60
[19] Galassi S 2008 Numerical analysis of masonry vaulted systems reinforced with composite materials (Dept. of Constructions, Florence, Italy)
[20] Galassi S 2018 Analysis of masonry arches reinforced with FRP sheets: experimental results and numerical evaluations *Key Eng. Mat.* (in press)
[21] Colonnetti G 1955 *Scienza delle Costruzioni* (Torino: Edizioni Scientifiche Einaudi)
[22] Coulomb C A 1776 Mémoires de mathématique et de physique présentés à l'Académie Royale des Sciences, par divers Savans, et Ius dans les Assemblées, Paris, Académie Royale des Sciences
[23] Gilbert M and Melbourne C 1994 Rigid-block analysis of masonry structures *Struct. Eng.* **72** 356-60
[24] Yuan H, Teng J C, Seracini R, Wu Z S and Yao J 2004 Full-range behavior of FRP-to-concrete bonded joints *Eng. Struct.* **26** 553-65
[25] Valluzzi M R, *et al* 2012 Round robin test for composite-to-brick shear bond characerization *Mater. Struct.* **45** 1761-91
[26] Rovero L, Focacci F and Stipo G 2013 Structural behavior of arch models strengthened using FRP strips of different lengths *J. Compos. Const.* **17** 249-58
[27] Rotunno T, Rovero L, Tonietti U and Briccoli Bati S 2015 Experimental study of bond behavior of CFRP-to-brick joints *J. Compos. Const* **19** 10.1061/(ASCE)CC.1943-5614.0000528, 04014063
[28] Briccoli Bati S and Rovero L 2008 Towards a methodology for estimating strength and collapse mechanism in masonry arches strengthened with fibre reinforced polymer applied on external surfaces *Mater. Struct.* **41** 1291-306